

# Accurate Crosstalk Analysis for RLC On-Chip VLSI Interconnect

Susmita Sahoo, Madhumanti Datta, Rajib Kar

**Abstract**—This work proposes an accurate crosstalk noise estimation method in the presence of multiple RLC lines for the use in design automation tools. This method correctly models the loading effects of non switching aggressors and aggressor tree branches using resistive shielding effect and realistic exponential input waveforms. Noise peak and width expressions have been derived. The results obtained are at good agreement with SPICE results. Results show that average error for noise peak is 4.7% and for the width is 6.15% while allowing a very fast analysis.

**Keywords**—Crosstalk, Distributed RLC segments, On-Chip Interconnect, Output response, VLSI, Noise Peak, Noise Width.

## I. INTRODUCTION

THE minimum feature size in VLSI circuits is shrinking; signal integrity issues gain importance due to increased coupling between nets in VLSI circuits, which results in crosstalk noise. Decreasing feature size affects the crosstalk noise problem and also affects the design's timing and functionality goals [1-2]. If the crosstalk effects on the victim net are large, they can propagate into storage elements that connect to victim line and can cause permanent errors. Several proposals have been made which model the crosstalk effects using simple lumped and/or distributed RC circuit models. Vittal [3] modeled each aggressor and victim net by a simple L-type lumped RC circuit and obtained a bound for crosstalk noise using a step input. Later extensions to this model are made in [4] and [5]; where a saturated ramp input or a  $\pi$ -type lumped RC circuit has been considered. Cong *et al.* later proposed a  $2\text{-}\pi$  model [6] that offered more accuracy than previous models. In this model, the victim line is modeled using the  $2\text{-}\pi$  model while the aggressor net is simplified as a saturated ramp at the coupling node. Later modifications are made to this model and an improved  $4\text{-}\pi$  model has been proposed [7]. In [7], the model [6] is extended to include the aggressor distributed line characteristics. However, the approach uses decoupling, and during the decoupling it ignores the victim loading effect on aggressor coupling node. Then a new approach in [8] was proposed based on  $4\text{-}\pi$  model

which was extension of [7]. It introduces a new multi-line model that considers non-switching aggressors as well as switching aggressors. With faster rise times and lower resistance, long wide wires in the upper metal layers exhibit significant inductive effects. An efficient resistance-inductance-capacitance (RLC) model of the on-chip interconnect is, therefore, critical in high level design, logic synthesis and physical design. A closed form expression for the cross-talk noise between two identical RLC lines is developed in [9], assuming that the two interconnects are loosely coupled. In [10], a technique to decouple coupled RLC interconnects into independent interconnects is developed based on a modal analysis. This decoupling method, however, assumes a TEM mode approximation, which is only valid in a two-dimensional structure with a perfect current return path in the ground plane directly beneath the conductors [11]. An estimate of crosstalk noise among multiple RLC interconnects is required to efficiently implement shielding techniques. Inserting shield lines can greatly reduce both capacitive coupling [12] and mutual inductive coupling by providing a closer current path for both the aggressor and victim lines. Dynamic crosstalk is discussed for coupled RLC interconnect in [17]. The proposal made in [18] presents a method to estimate the crosstalk from the output response using correlation method. Kim *et al.* [19] considers a linear driver model for the crosstalk calculation for RLC interconnects. In [20], closed form crosstalk modeling is proposed using matrix approximation. But these models either suffer from computational complexity or sacrifice the error by taking some approximations. This paper presents a closed form crosstalk analysis for inductively and capacitively coupled RLC interconnect based on  $4\text{-}\pi$  model. It considers the inductive effect and introduces a new multi-line model that considers non-switching aggressors as well as switching aggressors. The realistic exponential waveforms are considered during victim noise derivations. Our proposed crosstalk noise model is considerably different from the previous models as inductive coupling has been introduced between aggressor and victim lines along with capacitive coupling. It is also accurate in the respect that the passive aggressors are represented as equivalent capacitances to the victim line rather than simple lumped coupling capacitance. Equivalent capacitances represent the loading effect of passive aggressors on victim line and have been formulated by including realistic exponential aggressor waveform and resistive shielding. Similarly, the tree branches are also

Susmita Sahoo is with the Department of Electronics & Communication Engg., National Institute of Technology, Durgapur, West Bengal, 713029 (e-mail: susmitas1987@gmail.com).

Madhumanti Datta is with the Department of Electronics & Communication Engg., National Institute of Technology, Durgapur, West Bengal, 713029 (e-mail: madhumanti\_datta@rediffmail.com)

Rajib Kar is with the Department of Electronics & Communication Engg., National Institute of Technology, Durgapur, West Bengal, 713029 (e-mail: rajibkarece@gmail.com)

formulated by an equivalent capacitance. Based on this model, first aggressor coupling node waveform is derived. Then after calculating the transfer function between aggressor coupling node and victim receiver, victim noise waveform has been derived. Noise peak and width are the two parameters to determine whether the noise is below the acceptable limit. Therefore, the closed form analytic expressions for peak noise and noise width are also formulated. The results for different random circuits are compared with SPICE results. Simulations are also carried out for multiple switching aggressors and results show good agreement to HSPICE results.

II. THE 4- $\pi$  MODEL

The multi-line model has been developed based on 4- $\pi$  model parameters. In the 4- $\pi$  model, both victim and the aggressor net are modeled using the 2- $\pi$  circuits [7]. Finally, we obtain the template circuit, shown in Figure 1. In this model, effective resistances  $R_d$  and  $R_{th}$  model the victim and aggressor drivers, respectively. Drivers are represented by linear resistors, inductors and capacitors using the method described in [13]. The coupling node (node-2) is set to be the center of the coupling portion of the victim net.

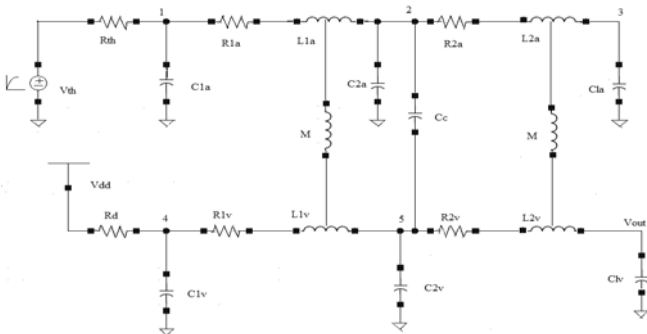


Fig. 1 The 4- $\pi$  model for two coupled interconnects

$R_{1a}$ ,  $L_{1a}$ ,  $C_{ua}$  are the upstream resistance, inductance and capacitance for the aggressor net, respectively. Similarly for victim net, let's assume upstream and downstream resistance, inductance, and capacitance at node 5 to be  $R_{1v}$ ,  $L_{1v}$ ,  $C_{uv}$  and  $R_{2v}$ ,  $L_{2v}$ ,  $C_{dv}$ , respectively. Then, for aggressor and the victim, we have:

$$C_{1a} = C_{ua}/2, C_{2a} = (C_{ua} + C_{da})/2 \text{ and } C_{3a} = C_{da}/2 + C_{lda}$$

$$C_{1v} = C_{uv}/2, C_{2v} = (C_{uv} + C_{dv})/2 \text{ and } C_{6v} = C_{dv}/2 + C_{ldv}$$

Here,  $C_{lda}$  and  $C_{ldv}$  represent the load capacitances for aggressor and victim lines, respectively.

III. PASSIVE AGGRESSOR MODELING BY EQUIVALENT CAPACITANCE

A victim can be coupled to many non-switching (passive) aggressors. In the earlier approaches the loading effect of a passive aggressor is simply taken as a coupling capacitor at victim coupling point [6-7]. However, a passive aggressor follows victim waveform and contributes to the stability of the victim line. Therefore, equivalent load capacitance at the

victim coupling point is less than the coupling capacitance and can be formulated using coupling and/or branching admittance concept as discussed in [14]. The inductance at node 1 of the aggressor will be the sum of two coupled inductance and twice the mutual inductance between them. In this paper, an equivalent capacitance formula for a passive aggressor is first derived assuming an exponential aggressor waveform. In order to derive the capacitance expression, the passive aggressor is first reduced to the simple circuit as shown in Figure 2b, where,

$$R'_a = R_{th} + R_{1a} \tag{1}$$

$$L'_a = L_{1a} + L_{1v} + 2M \tag{2}$$

$$C'_a = C_{2a} + C_{1a} + \left( \frac{R_{th}^2}{(R_{th} + R_{1a})^2} \right) C_{1a} \tag{3}$$

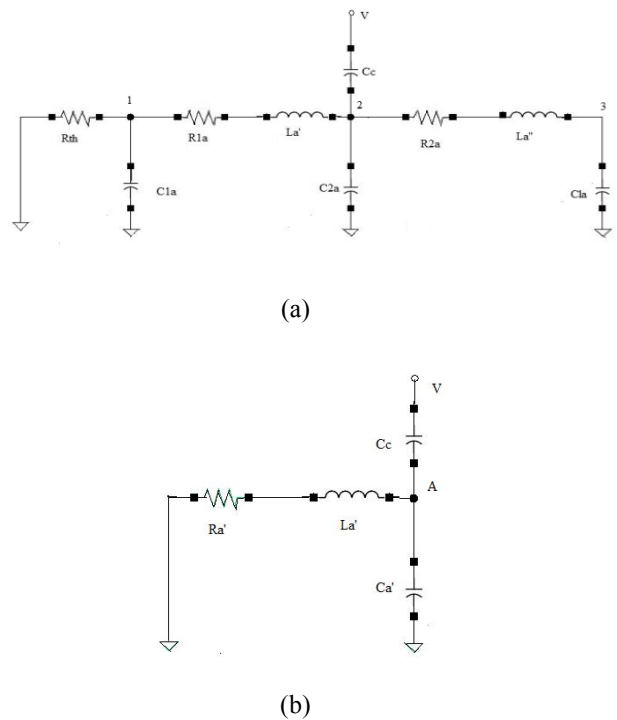


Fig. 2 A non-switching aggressor not coupled to the victim line

Then for matching purposes, the victim waveform is assumed to be a normalized exponential voltage, as shown in Figure-3. The equivalent capacitance for the passive aggressor can now be formulated.

The currents coming from the victim node should be same for both the cases and can be calculated as,

$$I = C_c \left[ \frac{dV_v(t)}{dt} - \frac{dV_A(t)}{dt} \right] = C_{eq} \frac{dV_v(t)}{dt} \tag{4}$$

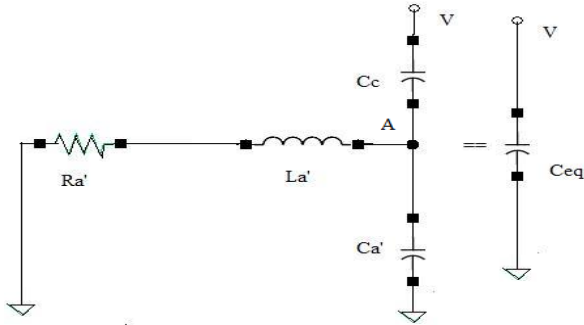


Fig. 3 Passive Aggressor line reduction

Assuming zero initial condition and exponential waveform, we can calculate the equivalent capacitance by integrating (4) over the interval  $0 \leq t \leq 5t_r$ . Here,  $t_r$  is the exponential rise time constant.

$$C_{eq} = C_c [1 - V_A(5t_r)] \quad (5)$$

Now considering left part of Figure-3,

$$C_c \left[ \frac{dV_v(t)}{dt} \right] = (C_c + C_a') \frac{dV_A(t)}{dt} + \frac{V_A(t)}{R_a'} + \frac{1}{L_a'} \int V_A(t) dt \quad (6)$$

Taking Laplace's transform of (6) yields,

$$V_A(s) \left[ sC_c + sC_a' + \frac{1}{R_a' + sL_a'} \right] = sC_c V_v(s) \quad (7)$$

$$\text{Now, } V_v(s) = \left( \frac{1}{s} - \frac{1}{s + \frac{1}{t_r}} \right) \quad (8)$$

$$\text{So, } V_A(s) = \frac{k \left( s + \frac{R_a'}{L_a'} \right)}{\left( s + \frac{1}{t_r} \right) \left[ s^2 + \left( \frac{R_a'}{L_a'} \right) s + \frac{1}{L_a' (C_c + C_a')} \right]} \quad (9)$$

$$\text{Where, } k = \frac{C_c}{t_r (C_c + C_a')} \quad (10)$$

Taking inverse Laplace's transform of (9),

$$V_A(t) = A_1 e^{-\frac{t}{t_r}} + A_2 e^{-\alpha t} + A_3 e^{-\beta t} \quad (11)$$

Where,  $\alpha, \beta, A_1, A_2, A_3$  are derived as follows:

$$\alpha = \frac{-R_a'}{2L_a'} + \sqrt{\left( \frac{R_a'}{2L_a'} \right)^2 - \frac{1}{L_a' (C_c + C_a')}} \quad (12)$$

$$\beta = \frac{-R_a'}{2L_a'} - \sqrt{\left( \frac{R_a'}{2L_a'} \right)^2 - \frac{1}{L_a' (C_c + C_a')}} \quad (13)$$

$$A_1 = \frac{kt_r (R_a' - L_a') (C_c + C_a')}{t_r^2 - R_a' t_r (C_c + C_a') + L_a' (C_c + C_a')} \quad (14)$$

$$A_2 = \frac{k (R_a' - \alpha L_a') t_r}{L_a' (1 - t_r \alpha) (\beta - \alpha)} \quad (15)$$

$$A_3 = \frac{k (R_a' - \beta L_a') t_r}{L_a' (1 - t_r \beta) (\alpha - \beta)} \quad (16)$$

Substituting the value of  $V_A(5t_r)$  in (5),  $C_{eq}$  can be represented as,

$$C_{eq} = C_c \left[ 1 - \left( A_1 e^{-\frac{5}{t_r}} + A_2 e^{-5\alpha} + A_3 e^{-5\beta} \right) \right] \quad (17)$$

A passive aggressor coupled to the victim line can be reduced to an equivalent capacitor using the formula derived above and this capacitor would then be taken in parallel with  $C_{2v}$  at node 5, the circuit would reduce to the one shown in Figure-1.

#### IV. RLC TREE AND BRANCH MODELING

The model proposed in [7] treats aggressor net branches simply as lumped capacitances at the branching point. However, the capacitance seen at the branching node is less than the total branch capacitance due to resistive shielding effect. Hence, the approach in [7] is incorrect. In this paper, an equivalent capacitance formula for tree branches is derived noting the exponential aggressor waveform. First, tree branches are reduced to a simple  $\pi$  model using the moment matching method as demonstrated in [14]. Then, this model reduces to an equivalent branching capacitance  $C_{eq-br}$  (Figure 4) considering an exponential waveform on input node A.

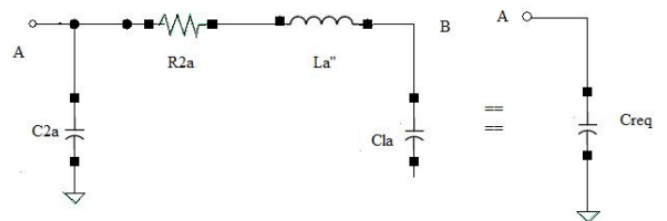


Fig. 4 Tree branch reduction on right part of aggressor net

In Figure-4, we can equate the currents in node A for both circuits:

$$C_{eq-br} \frac{dV_A(t)}{dt} = C_{2a} \frac{dV_A(t)}{dt} + C_{la} \frac{dV_B(t)}{dt} \quad (18)$$

Assuming a rising exponential voltage on input node and zero initial condition, we can obtain an equivalent branching capacitance after integrating both sides of above equation over  $0 \leq t \leq 5t_r$  time interval:

$$C_{eq-br} = C_{2a} + C_{la} V_B(5t_r) \quad (19)$$

Then by applying KCL on node B, one obtains the relation as given in (20).

$$\frac{V_A(s) - V_B(s)}{R_{2a} + L_a'' s} = s C_{la} V_B(s) \quad (20)$$

$$V_A(t) = 1 - e^{-\frac{t}{t_r}} \quad (21)$$

$$V_B(s) = \frac{\left( \frac{1}{t_r C_{la} L_a''} \right)}{s \left( s + \frac{1}{t_r} \right) \left( s^2 + \left( \frac{R_{2a}}{L_a''} \right) s + \frac{1}{C_{la} L_a''} \right)} \quad (22)$$

$$= \frac{A_4}{s} + \frac{A_5}{s + \frac{1}{t_r}} + \frac{A_6}{s + \alpha_1} + \frac{A_7}{s + \beta_1} \quad (23)$$

$$\text{Where, } \alpha_1, \beta_1 = \frac{-R_{2a}}{2L_a''} \pm \sqrt{\left( \left( \frac{R_{2a}}{2L_a''} \right)^2 - \frac{1}{C_{la} L_a''} \right)} \quad (24)$$

$$A_4 = 1 \quad (25)$$

$$A_5 = \frac{t_r^2}{-L_a'' C_{la} + R_{2a} C_{la} t_r - t_r^2} \quad (26)$$

$$A_6 = \frac{1}{\alpha_1 C_{la} L_a'' (1 - \alpha t_r) (\alpha_1 - \beta_1)} \quad (27)$$

$$A_7 = -\frac{1}{\beta_1 C_{la} L_a'' (1 - \beta_1 t_r) (\beta_1 - \alpha_1)} \quad (28)$$

Upon solving (23) and inserting  $t=5t_r$  yields,

$$V_B(t) = u(t) + A_5 e^{-\frac{t}{t_r}} + A_6 e^{-\alpha_1 t} + A_7 e^{-\beta_1 t} \quad (29)$$

$$V_B(5t_r) = u(5t_r) + A_5 e^{-\frac{5t_r}{t_r}} + A_6 e^{-5\alpha_1 t_r} + A_7 e^{-5\beta_1 t_r} \quad (30)$$

Finally, this value can be inserted in (19), which results,

$$C_{eq-br} = C_{2a} + C_{la} \left( u(t) + A_5 e^{-\frac{5t_r}{t_r}} + A_6 e^{-5\alpha_1 t_r} + A_7 e^{-5\beta_1 t_r} \right) \quad (31)$$

### V. AGGRESSOR WAVEFORM CALCULATION AT COUPLING NODE

Our proposed model uses a reduced transfer function between aggressor coupling node and the victim node, hence results in small accuracy loss compared to the method in [7]. In the previous work, the direct transfer function between aggressor input and victim output is first calculated, then dominant pole approximation is hired over the whole transfer function to reduce complexity. However, too much use of dominant pole approximation always reduces model accuracy.

In the proposed model, the aggressor waveform at the coupling node is first calculated and then entered to the transfer function between the coupling node and the victim output to obtain victim noise voltage. Compared to [7], the dominant pole approximation is used moderately which results in increased accuracy.

In order to model the coupling node aggressor waveform correctly, victim-loading effect on the aggressor node needs to be calculated. The loading effect is smaller than the coupling capacitor due to resistive shielding. The victim line can be reduced to an equivalent capacitor  $C_{eqv}$  using the quiet aggressor/victim net reduction techniques which are summarized in Section 3. The aggressor branches after the coupling point are also reduced to an equivalent capacitance  $C_{eq-br}$  using the tree branch reduction techniques discussed earlier.

After application of reduction techniques, the  $4-\pi$  network, shown in Figure 1, reduces to Figure 5 for aggressor coupling node voltage calculation.

From Figure-5,

$$V_1(s) = \frac{z}{z + R_{th}} V_{in}(s) \quad (32)$$

$$\text{Where, } \frac{1}{z} = \frac{1}{R_{1a} + sL_{eq} + \frac{1}{sC}} \quad (33)$$

$$\left. \begin{aligned} C &= C_{2a} + C_{eq-br} + C_{eqv} \\ L_{eq} &= L_{1a} + L_{1v} + L_{2a} + L_{2v} + 4M \end{aligned} \right\} \quad (34)$$

Then we have,

$$V_2(s) = \left( \frac{1}{L_{eq} C s^2 + R_{1a} C s + 1} \right) V_1(s) \quad (35)$$

$$V_2(s) = \left( \frac{1}{L_{eq} C s^2 + R_{1a} C s + 1} \right) \left( \frac{z}{z + R_{th}} \right) V_{in}(s) \quad (36)$$

Finally, the transfer function between the input and coupling node 2 can be derived as,

$$\frac{V_2(s)}{V_{in}(s)} = \frac{1}{L_{eq} C_{1a} C R_{th} s^3 + (R_{1a} C_{1a} R_{th} + L_{eq} C) s^2 + [(C_{1a} + C) R_{th} + R_{1a} C] s + 1} \quad (37)$$

Or, (38)

$$V_2(s) = \frac{\frac{1}{t_r}}{L_{eq}C_{1a}CR_{th}s^5 + \left(\frac{R_{1a}C_{1a}R_{th} + L_{eq}C}{t_r} + R_{1a}C_{1a}R_{th} + L_{eq}C\right)s^4 + \left[(C_{1a} + C)R_{th} + R_{1a}C + \frac{R_{1a}C_{1a}R_{th} + L_{eq}C}{t_r}\right]s^3 + \left(1 + \frac{(C_{1a} + C)R_{th} + R_{1a}C}{t_r}\right)s^2 + \frac{s}{t_r}}$$

The dominant pole approximation method [6] [15-16] is used to reduce the complexity of the transfer function. Finally we have,

$$V_2(s) = \frac{\frac{1}{t_r}}{s \left[ \left(\frac{a_2}{t_r} + a_1\right)s^2 + \left(\frac{a_1}{t_r} - 1\right)s + \frac{1}{t_r} \right]} \quad (39)$$

$$\left. \begin{aligned} a_1 &= [(C_{1a} + C)R_{th} + R_{1a}C] \\ \text{Where, } a_2 &= (R_{1a}R_{th}C_{1a} + L_{eq}C) \\ a_3 &= L_{eq}C_{1a}CR_{th} \end{aligned} \right\} \quad (40)$$

$$\text{Now } V_2(s) = \frac{A}{s} + \frac{B}{s + \alpha_2} + \frac{C}{s + \beta_2} \quad (41)$$

Where,

$$\alpha_2, \beta_2 = \frac{-\left(\frac{a_1}{t_r} + 1\right) \pm \sqrt{\left(\frac{a_1}{t_r} + 1\right)^2 - \frac{1}{t_r} \left(\frac{a_2}{t_r} + a_1\right)}}{2} \quad (42)$$

$$\left. \begin{aligned} A &= 1 \\ \text{and, } B &= \frac{1}{\alpha_2 t_r (\alpha_2 - \beta_2)} \\ C &= \frac{1}{\beta_2 t_r (\beta_2 - \alpha_2)} \end{aligned} \right\} \quad (43)$$

Taking inverse Laplace transform of (41),

$$V_2(t) = 1 + \frac{1}{t_r(\alpha_2 - \beta_2)} \left( \frac{1}{\alpha_2} e^{-\alpha_2 t} - \frac{1}{\beta_2} e^{-\beta_2 t} \right) \quad (44)$$

This waveform when plotted represents a delayed exponential waveform as expected. However, it contains two exponential terms, and should be reduced to only one term for simplicity. We assume the delayed waveform at coupling node to be

$$V_2(t) = 1 - e^{-\frac{t}{t_x}} \quad (45)$$

We equate these two waveforms from (44) and (45),

$$1 + \frac{1}{t_r(\alpha_2 - \beta_2)} \left( \frac{1}{\alpha_2} e^{-\alpha_2 t} - \frac{1}{\beta_2} e^{-\beta_2 t} \right) = 1 - e^{-\frac{t}{t_x}} \quad (46)$$

The area under both exponential terms should be same:

$$\text{So, } \frac{1}{t_r(\alpha_2 - \beta_2)} \left[ \int_0^\infty \frac{1}{\alpha_2} e^{-\alpha_2 t} dt - \int_0^\infty \frac{1}{\beta_2} e^{-\beta_2 t} dt \right] = - \int_0^\infty e^{-\frac{t}{t_x}} dt \quad (47)$$

$$\text{Or, } t_x = - \frac{t_r^2 \alpha_2^2 \beta_2^2}{\alpha_2 + \beta_2} \quad (48)$$

The new calculated rising exponential time constant  $t_x$  has been verified by plotting the function given in (45) simultaneously with HSPICE result. The following parameter values used for the verification:  $R_{th}=200$  Ohm,  $R_{1a}=R_{2a}=120$  Ohm,  $R_d=250$  Ohm,  $R_{1v}=R_{2v}=100$  Ohm. The coupling capacitance  $C_c$  is taken as 150fF. Other capacitances are given as follows:  $C_{ua}=C_{da}=100$  fF,  $C_{uv}=C_{dv}=100$  fF. Let the load capacitances for aggressor and victim line be 50 fF each.  $L_{1a}=L_{2a}=L_{1v}=L_{2v}=M=100$ nH. Also a normalized aggressor voltage is assumed and aggressor rise time  $t_r$  is chosen as 150 ps.

Figure 6 shows the result from HSPICE at aggressor coupling node. For the given parameter values above, the model predicts the new rise time constant ( $t_x$ ) as 20.967 $\mu$ Sec, while HSPICE calculates as 21.985 $\mu$ Sec. The model error is only 4.6%. For several random circuits, the model has been verified and error corresponding to each case is calculated and it has been found that the absolute error value remains less than 7%.

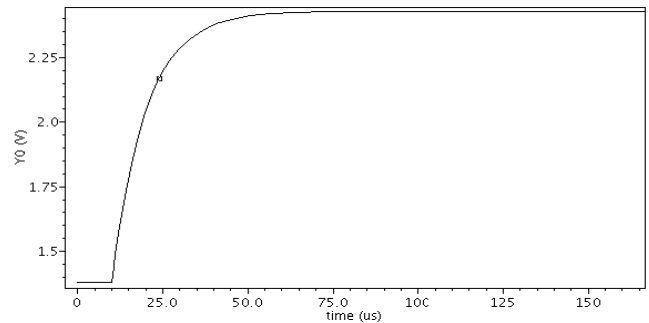


Fig. 6 Coupling point waveform of the aggressor

## VI. OUTPUT VOLTAGE FORMULATION

In the previous Section, the aggressor waveform at the coupling node is formulated by considering the exponential aggressor input. Now, the aggressor waveform at coupling location needs to be entered to the transfer function to calculate the noise as shown in Figure-7.

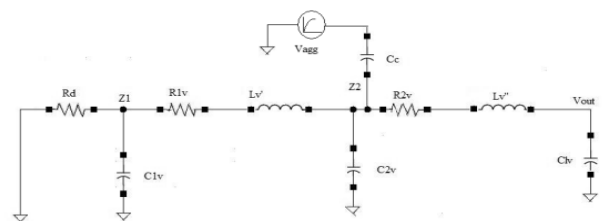


Fig. 7 Output voltage calculation

Referring to Figure-7 we have,

$$\frac{1}{z_1} = \frac{1}{R_d} + sC_{1v} \tag{49}$$

$$\frac{1}{z_2} = \frac{1}{R_{2v} + L_v''} + \frac{1}{sC_{lv}} + sC_{2v} + \frac{1}{z_1 + R_{1v} + sL_v'} \tag{50}$$

$$V_2(s) = \frac{z_2}{z_2 + \frac{1}{sC_c}} V_{agg}(s) \tag{51}$$

$$V_{noise}(s) = \frac{1}{C_{lv}L_v''s^2 + R_{2v}C_{lv}s + 1} V_2(s) \tag{52}$$

$$z_2 = \frac{a_4s^4 + a_3s^3 + a_2s^2 + a_1s + a_0}{b_5s^5 + b_4s^4 + b_3s^3 + b_2s^2 + b_1s + 1} \tag{53}$$

where,

$$a_4 = L_v' L_v'' C_{lv} C_{1v} R_d, a_3 = [L_v'' C_{lv} (L_v' + C_{1v} R_d R_{1v}) + L_v' C_{lv} C_{1v} R_d R_{2v}],$$

$$a_2 = [L_v'' C_{lv} (R_{1v} + R_d) + L_v' C_{lv} R_d + R_{2v} C_{lv} (L_v' + C_{1v} R_d R_{1v})]$$

$$a_1 = [L_v' + C_{1v} R_d R_{1v} + (R_{1v} + R_d) R_{2v} C_{lv}], a_0 = (R_{1v} + R_d)$$

$$b_5 = L_v' L_v'' C_{lv} C_{1v} R_d, b_4 = [L_v'' C_{lv} C_{2v} (L_v' + C_{1v} R_d R_{1v}) + L_v' C_{lv} C_{1v} C_{2v} R_d R_{2v}],$$

$$b_3 = [C_{lv} C_{2v} R_{2v} (L_v' + C_{1v} R_d R_{1v}) + (C_{lv} + C_{2v}) L_v' C_{1v} R_d],$$

$$b_2 = [(C_{lv} + C_{2v}) (L_v' + C_{1v} R_d R_{1v}) + (R_{1v} + R_d) C_{lv} C_{2v} R_{2v} + L_v'' C_{lv} + C_{lv} C_{1v} R_d R_{2v}]$$

$$b_1 = [(R_{1v} + R_d) (C_{lv} + C_{2v}) + R_{2v} C_{lv} + C_{1v} R_d]$$

Applying the value of  $z_2$  in (51),

$$\frac{V_{noise}(s)}{V_{agg}(s)} = \frac{sC_c(a_4s^4 + a_3s^3 + a_2s^2 + a_1s + a_0)}{(C_{lv}L_v''s^2 + R_{2v}C_{lv}s + 1) \left[ \begin{matrix} (C_c a_4 + b_5)s^5 + \\ (C_c a_3 + b_4)s^4 + \\ (C_c a_2 + b_3)s^3 \\ + (C_c a_1 + b_2)s^2 \\ + (C_c a_0 + b_1)s + 1 \end{matrix} \right]} \tag{54}$$

The Dominant Pole Approximation method [6] [15-16] is used in the above equation to reduce the complexity of the transfer equation. Finally we have,

$$\left. \begin{aligned} \frac{V_{noise}(s)}{V_{agg}(s)} &= \frac{C_c s(a_1s + a_0)}{p_2s^2 + p_1s + 1} \\ \text{where,} \\ p_2 &= [C_{lv}L_v'' + (C_c a_0 + b_1)R_{2v}C_{lv} + (C_c a_1 + b_2)] \\ p_1 &= [(C_c a_0 + b_1) + R_{2v}C_{lv}] \end{aligned} \right\} \tag{55}$$

If we insert the exponential function in (44) as the aggressor voltage, we obtain the following noise waveform:

$$V_{noise}(s) = \left( \frac{C_c s(a_1s + a_0)}{p_2s^2 + p_1s + 1} \right)^* \left[ \frac{1}{t_r} \right] \left[ \frac{1}{s \left[ \left( \frac{a_2}{t_r} + a_1 \right) s^2 + \left( \frac{a_1}{t_r} - 1 \right) s + \frac{1}{t_r} \right]} \right] \tag{56}$$

Again applying dominant pole approximation method to the above equation, it becomes,

$$V_{noise}(s) = \frac{C_c}{t_r} (a_1s + a_0) \frac{1}{\left[ \left( \frac{a_2}{t_r} + a_1 \right) + \left( \frac{a_1}{t_r} + 1 \right) p_1 + \frac{p_2}{t_r} \right] s^2 + \left[ \left( \frac{p_1}{t_r} + \frac{a_1}{t_r} + 1 \right) s + \frac{1}{t_r} \right]} = \frac{A_8}{s + \alpha_3} + \frac{A_9}{s + \beta_3} \tag{57}$$

where,

$$\alpha_3, \beta_3 = -\frac{\left( \frac{p_1}{t_r} + \frac{a_1}{t_r} + 1 \right)}{2} \pm \sqrt{\left[ \left( \frac{p_1}{t_r} + \frac{a_1}{t_r} + 1 \right)^2 - \left[ \left( \frac{a_2}{t_r} + a_1 \right) + \left( \frac{a_1}{t_r} + 1 \right) p_1 + \frac{p_2}{t_r} \right] \frac{1}{t_r}} \right]} \tag{58}$$

Applying inverse Laplace transform to (58), we will get,

$$V_{noise}(t) = A_8 e^{-\alpha_3 t} + A_9 e^{-\beta_3 t} \tag{60}$$

where,

$$A_8 = \frac{C_c}{t_r} \frac{(a_0 - a_1 \alpha_3)}{\beta_3 - \alpha_3}, \quad A_9 = \frac{C_c}{t_r} \frac{(a_0 - a_1 \beta_3)}{\alpha_3 - \beta_3} \tag{61}$$

$$\text{So, } V_{noise}(t) = \frac{C_c}{t_r (\beta_3 - \alpha_3)}^* \left[ (a_0 - a_1 \alpha_3) e^{-\alpha_3 t} - (a_0 - a_1 \alpha_3) e^{-\beta_3 t} \right] \tag{62}$$

By differentiating  $V_{noise}(t)$  with respect to  $t$ , the time when the noise voltage reaches its peaks,  $t_{peak}$ , can be found:

$$\frac{dV_{noise}(t)}{dt} = 0 \tag{63}$$

$$t_{peak} = \frac{1}{\alpha_3 - \beta_3} \ln \left[ \frac{\alpha_3(a_0 - a_1\alpha_3)}{\beta_3(a_0 - a_1\beta_3)} \right]$$

The noise peak voltage  $V_{peak}$  is found by substituting (63) in (62):

$$V_{peak}(t) = \frac{C_c}{t_r(\beta_3 - \alpha_3)} \left[ \left( (a_0 - a_1\alpha_3) \left[ \frac{\alpha_3(a_0 - a_1\alpha_3)}{\beta_3(a_0 - a_1\beta_3)} \right]^{\frac{\alpha_3}{\alpha_3 - \beta_3}} \right) - \left( (a_0 - a_1\beta_3) \left[ \frac{\alpha_3(a_0 - a_1\alpha_3)}{\beta_3(a_0 - a_1\beta_3)} \right]^{\frac{\beta_3}{\alpha_3 - \beta_3}} \right) \right] \tag{64}$$

Noise peak has been traditionally used as a metric to determine whether the noise is at an acceptable level. However, the noise width is also a necessary metric in determining whether a noise pulse can go through a receiver. If noise peak exceeds the threshold, but does not carry sufficient width, the noise may not be received at the receiver output at all. Therefore, the noise width should also simultaneously be considered. The noise peak expression is derived in (64). For noise width, the threshold is usually taken as 50% of  $V_{peak}$ . Considering (62) and the threshold, one can obtain a function  $f(t)$  which can be used in Newton's Iteration method to solve for  $t_1$  and  $t_2$  time instances.

$$\frac{C_c}{t_r(\beta_3 - \alpha_3)} \left[ (a_0 - a_1\alpha_3)e^{-\alpha_3 t} - (a_0 - a_1\beta_3)e^{-\beta_3 t} \right] = \frac{0.5C_c}{t_r(\beta_3 - \alpha_3)} \left[ \left( (a_0 - a_1\alpha_3) \left[ \frac{\alpha_3(a_0 - a_1\alpha_3)}{\beta_3(a_0 - a_1\beta_3)} \right]^{\frac{\alpha_3}{\alpha_3 - \beta_3}} \right) - \left( (a_0 - a_1\beta_3) \left[ \frac{\alpha_3(a_0 - a_1\alpha_3)}{\beta_3(a_0 - a_1\beta_3)} \right]^{\frac{\beta_3}{\alpha_3 - \beta_3}} \right) \right] \tag{65}$$

Where,

$$f(t) = (a_0 - a_1\alpha_3) \left( e^{-\alpha_3 t} - 0.5 \left[ \frac{\alpha_3(a_0 - a_1\alpha_3)}{\beta_3(a_0 - a_1\beta_3)} \right]^{\frac{\alpha_3}{\alpha_3 - \beta_3}} \right) - (a_0 - a_1\beta_3) \left( e^{-\beta_3 t} - 0.5 \left[ \frac{\alpha_3(a_0 - a_1\alpha_3)}{\beta_3(a_0 - a_1\beta_3)} \right]^{\frac{\beta_3}{\alpha_3 - \beta_3}} \right) \tag{66}$$

And,

$$f'(t) = \beta_3(a_0 - a_1\beta_3)e^{-\beta_3 t} - \alpha_3(a_0 - a_1\alpha_3)e^{-\alpha_3 t} \tag{67}$$

This method converges vary rapidly if the initial guesses are taken carefully. The initial guesses of  $t_1$  and  $t_2$  are taken as

$\frac{1}{4} t_{peak}$  and  $4t_{peak}$ , respectively. The values of  $t_1$  and  $t_2$  are updated using the iteration formula given below:

$$t_{1_{k+1}} = t_{1_k} - \frac{f(t_{1_k})}{f'(t_{1_k})} \tag{68}$$

$$\text{and, } t_{2_{k+1}} = t_{2_k} - \frac{f(t_{2_k})}{f'(t_{2_k})} \tag{69}$$

Then, the noise width is defined by,

$$t_{width} = t_2 - t_1 \tag{70}$$

The algorithm converges very rapidly after some iteration.

### VII. VALIDATION OF THE PROPOSED MODEL

The model has been tested extensively and its accuracy has been compared with SPICE simulation results. Several circuits with different parameter values have been taken and tested. The parameter ranges were taken as follows:  $R_d$  and  $R_{th}$  are 10-1500Ω; load capacitances for victim and aggressor lines are 5-50 fF; aggressor and victim wire resistances are 10-250 Ohms; aggressor and victim line capacitances are 0.5-100 nH; the mutual inductance between aggressor and victim are 150 nH and finally  $t_r$  is chosen in the range between 20-500 ps. After substituting these values in (64) and (70), noise peak and width have been calculated. In Table-1, noise peak and noise width of the proposed model is compared with SPICE result, and the average error for noise peak is found to be 4.707% and for noise width 6.1523%.

TABLE I  
EXPERIMENTAL RESULTS FOR NOISE PEAK AND NOISE WIDTH

Sr. No.	$T_r$ (psec)	$R_d/R_{th}$ (Ohm)	$R_{1a}/R_{2a}/R_{1v}/R_{2v}$ (Ohm)	$L_{1a}/L_{2a}/L_{1v}/L_{2v}$ (nH)	$C_{1a}/C_{1v}$ (fF)	$V_{peak}$ (SPICE) (mV)	$V_{peak}$ (Proposed Model) (mV)	Relative Error (%)	$T_{width}$ (SPICE) ( $\mu$ Sec)	$T_{width}$ (Proposed Model) ( $\mu$ Sec)	Relative Error (%)
1	50	10	10	0.5	5	912.982	861.8959	5.5953	1.222	1.1463	6.21
2	100	50	20	1.0	10	912.989	866.2354	5.12	1.289	1.2056	6.5
3	150	100	50	10	15	912.996	860.857	5.71	2.13157	2.00798	5.798
4	200	150	70	20	20	913.997	864.3669	5.43	2.42145	2.28066	5.814
5	250	200	100	30	25	913.998	868.471	4.98	2.727	2.5398	6.89
6	300	250	120	40	30	914.929	871.7571	4.71	2.884	2.716	5.81
7	350	500	150	50	35	914.934	873.4232	4.537	2.9595	2.7775	6.15
8	400	750	170	60	40	914.983	879.5815	3.869	3.2041	3.0129	5.97
9	450	1000	200	70	45	914.995	881.673	3.642	3.2941	3.072	6.75
10	500	1500	250	100	50	914.998	883.14	3.482	3.3615	3.1726	5.631

TABLE I  
EXPERIMENTAL RESULTS OBTAINED FOR MULTIPLE AGGRESSOR LINES COUPLED TO VICTIM LINE

No of aggressors	Noise Peak (Volt) SPICE Result	Noise Peak (Volt) Estimated Value	Relative error (%)	Noise Width (m Sec) SPICE Result	Noise Width (mSec) Estimated	Relative error (%)
1	0.914934	0.8734232	4.537	2.9595	2.7775	6.15
2	1.8432	1.7468	5.23	5.8615	5.555	5.23
3	2.7571	2.620	4.961	8.767	8.3325	4.956
4	3.669	3.493	4.79	11.6689	11.11	4.789
5	4.594	4.3671	4.95	14.611	13.8875	4.95

VIII. MULTIPLE ACTIVE AGGRESSORS

In a real circuit, a given victim line can be coupled to many switching aggressors. In this case, superposition theorem can be applied to calculate the total cross-coupling noise. With superposition, each active aggressor is switched at a time while holding other aggressor drivers quiet. The noise contributions are summed at the end to calculate total noise at the victim end. If there are N switching aggressors, it is necessary to calculate noise for N times to obtain the final result, hence time complexity is linear. Prior to any noise calculation, an equivalent capacitance value should be calculated for each aggressor using (17). The equivalent capacitance values are utilized for superposition to represent non-switching aggressors and this reduces the complex multi-line network into a manageable 4- $\pi$  template shown in Figure-1 during each superposition step. Table-II shows experimental results obtained for multiple aggressors' case. Experiments are performed upto 5 aggressors.  $R_d/R_{th}=500\Omega$ ,  $R_{1a}=R_{2a}=R_{1v}=R_{2v}=150\Omega$ ,  $L_{1a}=L_{2a}=L_{1v}=L_{2v}=50nH$ ,  $M=150nH$ ,

$C_{1a}=C_{1v}=50fF$ . The noise peak and width values of the previous approach in [7] are used, and the proposed approach has been compared with SPICE simulation results. The proposed approach has an average error of 4.89% for the noise peak and 5.215% for the noise width. The inclusion of victim loading effect, the equivalent capacitance representation for passive aggressors and moderate use of dominant pole approximation method makes our approach superior in terms of accuracy.

IX. CONCLUSION

This paper presents a new improved model for crosstalk noise estimation of two or multiple RLC interconnects using 4- $\pi$  model with less than 6% error on average compared with SPICE simulation, for both noise peak and width estimation. It also estimates crosstalk noise in the presence of multiple aggressor lines correctly. The proposed model presents a complete multi-line noise model by representing active and passive aggressors simultaneously. For passive aggressors, an equivalent capacitance model has been derived noting realistic

exponential aggressor waveform and formulation included resistive shielding effects. Then closed form expression for noise peak and width has been derived and compared against SPICE results and results are very promising. Results show that the average error for noise peak is 4.89% and for the noise width is 5.2% while allowing very fast analysis time. This  $4-\pi$  model will be useful in many applications at various levels to guide noise aware DSM circuit designs.

[20] Roy S, Dounavis A. "Closed form delay and crosstalk models for RLC on-chip interconnects using a matrix rational approximations". IEEE transactions on Computer Aided Design of integrated circuits and systems, vol. 28, issue. 10, pp. 1481-1492, October, 2009.

#### REFERENCES

- [1] Semiconductor Industry Association, National Technology Roadmap for Semiconductors, 1997.
- [2] Shepard K L, Narayanan V. "Noise in deep submicron digital design". Proc. IEEE Int. Conference on Computer Aided Design, pp. 524-531, 1996.
- [3] Vittal A, and M. Marek-Sadowska, "Crosstalk reduction for VLSI", IEEE Transactions on Computer-Aided Design, Vol. 16, pp. 1817-1824, 1997.
- [4] Kahng A B, Muddu S, Vidhani D. "Noise and delay uncertainty studies for coupled RC interconnections". IEEE Int. ASIC/SOC Conf., pp. 3-8, 1999.
- [5] Nakagawa S, Sylvester D M, McBride J, Oh S Y. "On-Chip crosstalk noise model for deep sub micrometer ULSI interconnect". Hewlett Packard Journal, Vol. 49, pp.39-45, 1998.
- [6] Cong J, Pan D Z, Srinavas P V. "Improved crosstalk modeling for noise constrained interconnect optimization". Proceedings of ASP/DAC, pp. 373-378, 2001.
- [7] Becer M R, Blaauw D, Zolotov V, Panda R, Hajj I N. "Analysis of noise avoidance techniques in DSM interconnects using a complete crosstalk noise model", Design, Automation and Test in Europe Conference, pp. 456-464, 2002.
- [8] Sayil S, Rudrapati M. "Accurate prediction of crosstalk for RC Interconnect". Turk J. Elec. Eng. and Comp Science, Vol.17, No.1, 2009, pp. 55-67.
- [9] Tang K T, Friedman E G. "Peak crosstalk noise estimation in CMOS VLSI circuits". in Proc. IEEE Int. Conf. Electron. Circuits Syst., pp. 1539-1542, 1999.
- [10] Chen J, He L. "A decoupling method for analysis of coupled RLC interconnects". in Proc. ACM Great Lakes Symp. VLSI, pp.41-46,2002.
- [11] Jin W, Yoon S, Kim J. "Experimental characterization and modeling of transmission line effects for high speed VLSI circuit interconnects". Inst. Electron. Informat. Commun. Eng. Trans. Electron., vol.83, no. 5, pp. 728-735, May 2000.
- [12] Zhang J, Friedman E G. "Crosstalk noise model for shielded interconnects in VLSI based circuits," in Proc. IEEE Int. SOC Conf., pp.243-244, 2003.
- [13] Levy R, Blaauw D, Braca G, Dasgupta A, Grinshpon A, Oh C, Orshav B, Sirichotiyakul S, Zolotov V. "Clarinet: A noise analysis tool for deep submicron design". in Proc. Int. Conf. Computer-Aided Design, pp. 587-594, Nov. 2002.
- [14] Qian J, Pulella S, Pillage L T. "Modeling the effective capacitance for the RC interconnect of CMOS gates". IEEE Transactions on Computer-Aided Design, Vol. 13, pp. 1526-1535, 1994.
- [15] Pillage L T, and Rohrer R A. "Asymptotic Waveform Evaluation for Timing Analysis". IEEE Transactions on Computer-Aided Design, Vol. 9, No. 4, pp. 352 - 366, 1990.
- [16] Acar E, Odabasioglu A, Celik M, and Pileggi L. "S2p: a stable 2- pole RC delay and coupling noise metric IC interconnects". Proceedings 9th Great Lakes Symposium on VLSI, pp. 60-63, 1999.
- [17] Kausik B K, Sarkar S, Agarwal R P, Joshi R C, "An analytical approach to dynamic crosstalk in coupled interconnects". Microelectronics journal, 41 (2010), pp. 85-92.
- [18] Lorival J E, Deschacht D. "RLC Interconnect crosstalk waveform evaluation". 2007 IEEE international Symposium on Integrated Circuits (ISIC 2007), pp. 544-547,2007.
- [19] Kim T, Kim D, Lee J, Eo Y. "Compact models for signal transient and crosstalk noise of coupled RLC interconnect lines with ramp input". 4<sup>th</sup> IEEE International Symposium on electronic design, test and applications, pp. 205-209, 2008.